

# Waveguide biosensor with integrated detector array for tuberculosis testing

Rongjin Yan,<sup>1,a)</sup> N. Scott Lynn,<sup>2</sup> Luke C. Kingry,<sup>3</sup> Zhangjing Yi,<sup>1</sup> Richard A. Slayden,<sup>3</sup> David S. Dandy,<sup>2,4</sup> and Kevin L. Lear<sup>1,4</sup>

<sup>1</sup>Department of Electrical and Computer Engineering, Colorado State University, Colorado 80523-1373, USA

<sup>2</sup>Department of Chemical and Biological Engineering, Colorado State University, Colorado 80523-1370, USA

<sup>3</sup>Department of Microbiology, Immunology, and Pathology, Colorado State University, Colorado 80523-2025, USA

<sup>4</sup>School of Biomedical Engineering, Colorado State University, Colorado 80523-1376, USA

(Received 27 August 2010; accepted 3 November 2010; published online 4 January 2011)

A label-free immunoassay using a local evanescent array coupled (LEAC) biosensor is reported. Complementary metal oxide semiconductor chips with integrated photoconductor arrays are used to detect an antibody to a *M. tuberculosis* protein antigen, HspX. The metrology limits of the LEAC sensor using dc and ac measurement systems correspond to average film thicknesses of 28 and 14 pm, respectively. Limits of detection are 87 and 108 pm, respectively, for mouse immunoglobulin G antibody patterning and antigen detection.

© 2011 American Institute of Physics. [doi:10.1063/1.3520142]

Tuberculosis (TB) is one of the most widespread infectious diseases in the world and a leading cause of death, as the World Health Organization estimates  $1.3 \times 10^6$  people died from TB in 2008. Improved point-of-care diagnostic modalities could dramatically boost prevention efforts and enable the appropriate drug regimen to be prescribed during the same patient visit. Conventional TB diagnostic methods, such as bacteriological culture and radiographic methods, are expensive and time-consuming. Less expensive methods, such as the TB skin (PPD) test, cannot effectively differentiate among disease states, including recent exposure, latent infection, or drug resistant TB variants.<sup>1,2</sup> An ideal TB diagnostic device would be portable, affordable, robust, and have the ability to differentiate disease states in near real-time.

The local evanescent array coupled (LEAC) sensor is a promising platform for point-of-care TB diagnostics. The sensor fabrication is compatible with trailing-edge complementary metal oxide semiconductor (CMOS) technology, which both lowers its cost and makes it possible to build a portable lab-on-a-chip system with silicon integrated circuits. As a label-free optical biosensor, it does not require reagents during testing. Furthermore, the LEAC approach is less sensitive to temperature or wavelength variations than resonance-based label-free optical biosensors,<sup>3,4</sup> or ring resonator biosensors.<sup>5</sup> Molecular specificity is provided by probe molecules, e.g., monoclonal- or monospecific polyclonal antibodies, immobilized on the sensor during the manufacturing process.

The physical principle underpinning LEAC sensor operation is the local field shift mechanism, as shown in Fig. 1(a). The increase of effective refractive index above the waveguide due to an increase in nanobiofilm thickness causes the evanescent field distribution to shift upwards into the nanobiofilm, which decreases the photocurrent through

the buried detector.<sup>6</sup> The field shift mechanism, in a proof-of-concept configuration without buried detector arrays, was validated with near field scanning optical microscopy on inorganic adlayers,<sup>7</sup> photoresist,<sup>8</sup> and different concentrations of C-reactive protein.<sup>9</sup> The LEAC sensor with buried detector arrays has been tested using patterned single layer organic films, including photoresist and bovine serum albumin (BSA).<sup>6,10</sup> In this paper, the immunoassay capabilities of the LEAC sensor are tested with immunoassay complexes, including mouse derived immunoglobulin G (IgG) and the *M. tuberculosis* antigen HspX.

The LEAC biosensor chips used in this study were fabricated with commercial 0.35  $\mu\text{m}$  CMOS technology as previously described.<sup>10</sup> For measurements, 654 nm laser light was coupled into the waveguide using end-fire coupling through a single mode fiber (4/125  $\mu\text{m}$  core/cladding diameter). The dc photocurrents in an anti-IgG experiment were measured using a Keithley 2400 source meter. An ac measurement system was used in an HspX experiment with a 16.8 Hz, 3 V peak-to-peak ac signal and 2.6 V offset from a

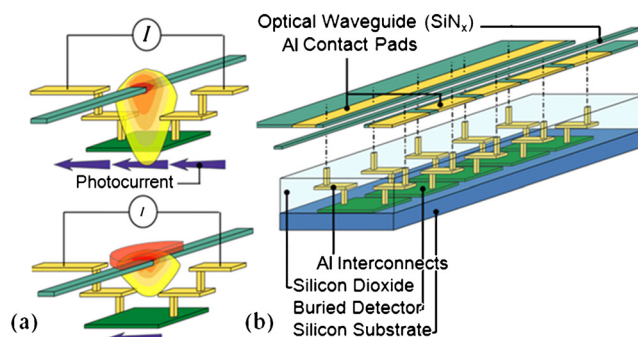


FIG. 1. (Color online) (a) LEAC sensor concept: the E-field shifts up when light propagates into a waveguide region covered by a nanofilm. Immobilization of molecular probes such as antibodies on the waveguide surface allows specific detection of target molecules such as antigens via affinity interactions. (b) The structure of the LEAC biosensor chip used in this paper.

<sup>a)</sup>Electronic mail: yanrj@engr.colostate.edu.

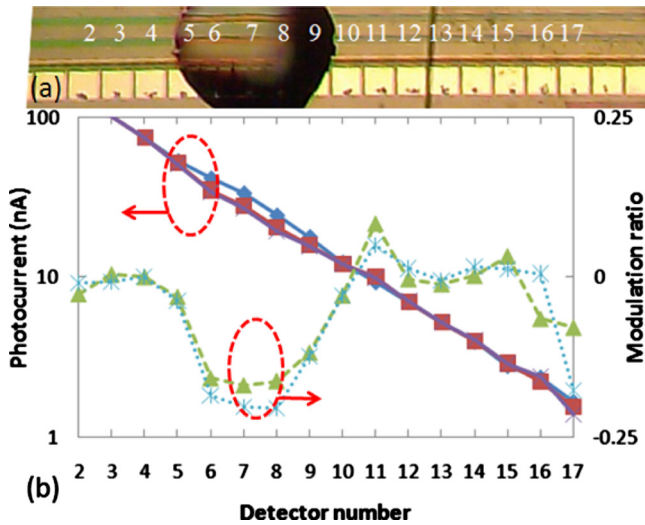


FIG. 2. (Color online) (a) Microscope image of a LEAC sensor chip with goat antimouse IgG solution printed above detectors 5 through 9 before rinsing. Since the capture antibodies were not fluorescently labeled, the patterned spot, which was  $\sim 1$  nm thick after rinsing and drying, could not be observed under an optical microscope. The detector pitch is  $100 \mu\text{m}$ . (b) Photocurrents measured before (blue diamonds) and after the goat antimouse IgG (red squares) /mouse IgG (crosses) was patterned as well as the respective current ratios (triangles and stars).

HP8116A function generator to both modulate the laser diode and serve as the reference signal for the lock-in amplifier. A PAR-5210 dual-phase lock-in amplifier measured the photocurrents. Signal from a third needle probing a fixed pad was used to normalize the signal collected from other pads, to account for change in the coupled power resulting from fiber movement. After drying with nitrogen, the samples were exposed to room air for 2 h before the measurement in order to partially stabilize the accumulation of any water film on the sensor surface.<sup>11</sup>

The immunosensing ability of the LEAC sensor was tested as follows: A microarray printer (BioRad VersArray ChipWriter Pro) printed a solution of goat antimouse IgG ( $200 \text{ ng}/\mu\text{l}$ , Invitrogen) in a  $\sim 500 \mu\text{m}$  diameter spot isolated on the waveguide above detectors 5 to 9 [Fig. 2(a)]. After a 20 min incubation to allow for covalent protein immobilization onto the waveguide, the sample was rinsed with de-ionized (DI) water and dried with nitrogen gas. Next, the baseline photocurrent distribution was measured, after which the microarray printer was used to deliver a solution of mouse IgG ( $100 \text{ ng}/\mu\text{l}$ ) to the same position. Following another 20 min incubation, rinsing and drying procedure, the final photocurrent through each detector was measured.

Figure 2(b) displays the photocurrent  $I$  and modulation ratio  $\Delta I/I_0$  for each of the 16 photodetectors along the waveguide. As expected, incubation with the target solution decreased the measured photocurrent under the probe spot due to specific binding of the target antigen. On detectors 6–8, 16.3% average modulation ratio was observed due to the presence of the goat anti-mouse IgG (antibody) patterning. An additional 3.5% decrease in photocurrent was detected after the mouse IgG (antigen) incubation, indicating an increase in the overall thickness of the protein nanobiofilm. As previously discussed,<sup>10</sup> smaller modulation ratios on the first and the last detectors are attributed to scattering at the boundaries of the patterned region. Maximizing binding site density by optimizing antibody immobilization conditions

would improve the modulation ratios, and thus the performance of the platform.<sup>12</sup>

The observed variability in the readings of the LEAC sensor results from a combination of noise from the optoelectronic system, variation in the sensitivity of individual detectors, and variation in the average thickness of the immobilized biofilms. To estimate the effects of the first factor, the current on one detector was measured 100 times over 10 s. The standard deviation ( $SD$ ) of the photocurrent, which is the difference between the total current with light,  $I_{\text{coupled}}$ , and the dark current  $I_{\text{dark}}$ , is  $SD(I) = \sqrt{SD(I_{\text{coupled}})^2 + SD(I_{\text{dark}})^2}$ . The typical  $SD$  of both the coupled and dark currents from 100 dc measurements was 60 pA. The dark and light coupled total currents were usually 1–10 nA, which gives a shot noise limit of 90–290 fA an integration time of 16.7 ms. The measurement noise is about 200 times the shot noise limit and likely due to instrumentation noise or polysilicon grain boundary trap-induced telegraph noise. Laser diode relative intensity noise was suppressed by the use of a reference channel. The current modulation ratio of the  $j$ th detector for a change in film thickness  $\Delta d = d_1 - d_0$  is defined as  $M_j(\Delta d) = 1 - [I_j(d_1)I_{\text{ref}}(d_0)]/[I_j(d_0)I_{\text{ref}}(d_1)]$ , where  $I_j(d)$  is the photocurrent of the  $j$ th detector with the nanofilm average thickness of  $d$ , and  $I_{\text{ref}}$  is the photocurrent from the reference detector, which is used to normalize the currents from different measurements. The  $SD$  of the current modulation ratio due to the optoelectronic system noise  $\sigma_{\text{oe}}$  is  $\sigma_{\text{oe}} = (1 - M_j) \sqrt{\text{RSD}_j(d_1)^2 + \text{RSD}_j(d_0)^2 + \text{RSD}_{\text{ref}}(d_0)^2 + \text{RSD}_{\text{ref}}(d_1)^2}$ , where  $\text{RSD}_j(d) = SD(I_j)/I_j$  is the relative standard deviation. The standard error of the current modulation ratio due to optoelectronic noise,  $SE_{\text{oe}} = \sigma_{\text{oe}}/\sqrt{N}$ , was calculated to be 0.23% from 100 samples, which required a total of 10 s of acquisition time for each measured current. The t-value is 1.98 for a 95% confidence interval. The average sensitivity  $S$  of the LEAC sensor with a core thickness of 100 nm used in this experiment is 16%/nm as determined from previous experiments and simulations.<sup>7</sup> The metrology limit (t-value  $\times SE_{\text{oe}}$ ) is 0.46% for dc measurement, corresponding to 28 pm.

To estimate the limit of detection (LOD) of the LEAC sensor, the sensitivity variations and the average thickness difference of the immobilized nanobiofilm on different detectors were considered. The  $SD$  of the current modulation ratios from  $N=3$  different detectors (detector 6–8),  $\sigma_{\text{total}} = SD[M_j(\Delta d)] = \sqrt{1/N \times \sum_{j=1}^3 [M_j(\Delta d) - \bar{M}(\Delta d)]^2}$ , in the patterned region with nominally identical nanofilm are used to estimate the LOD.<sup>15</sup> After the goat antimouse IgG patterning and the mouse IgG incubation, the standard error of the average current modulation ratio,  $SE_{\text{total}} = \sigma_{\text{total}}/\sqrt{3}$ , on the three detectors is 0.32% and 0.4%, respectively. For three samples, the t-value is 4.3 for a 95% confidence interval. The LOD, defined as t-value  $\times SE_{\text{total}}$ , is 1.39% and 1.74%, respectively, corresponding to 87 pm for the antibody patterning and 108 pm for the bound antigen layer. This LOD accounts for the three sources of variation mentioned above, i.e., system noise, detector-to-detector variation in sensitivity, and variations in the effective thickness of the nanobiofilms. The latter two were not separated in the experiments here, although the detector-to-detector sensitivity variation is assumed to be small for detectors that are in close proximity. The system

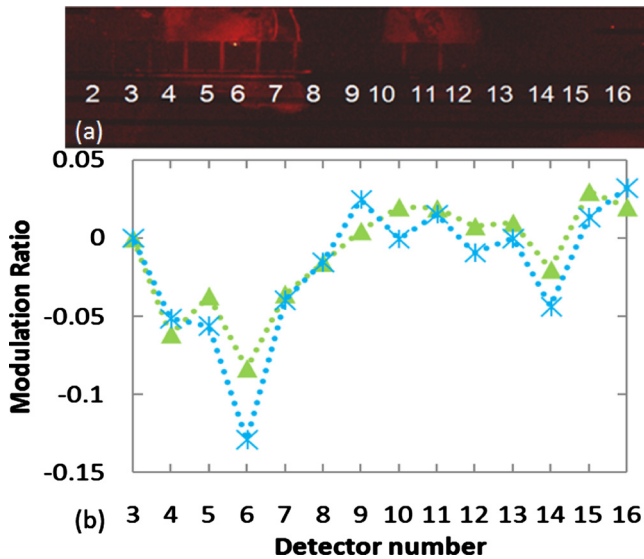


FIG. 3. (Color online) (a) Fluorescent intensity image of a LEAC sensor waveguide with an HspX antigen-antibody complex patterned above the detector 4 through 7 and antigen 85 spot over detectors 10 through 13. (b) Measured current modulation ratios after anti-HspX (triangle) and anti-mouse IgG (star).

noise, 0.23%, was 1/2 to 2/3 of  $\sigma_{\text{total}}$  the total standard deviation implying that the normalized variation in film thickness was comparable to or greater than the system noise associated with dc measurements.

The specificity of the LEAC biosensor was investigated in a manner characteristic of traditional diagnostic procedures for serology. *M. tuberculosis* protein antigens Ag85 and HspX were utilized as capture probes for detection of disease specific antibodies.<sup>13</sup> After a sample surface treatment to improve probe immobilization,<sup>14</sup> the microarray printer was used to print the two antigens (200 ng/ $\mu\text{L}$ ) in two separate locations along the waveguide, each with a spot diameter of  $\sim 400 \mu\text{m}$ . The prepared LEAC sensor sample was then incubated in 60% humidity for 20 min before being rinsed with DI water and dried. Next, the sample was submerged into a 10 % BSA solution for 1 h to passivate the remaining unpatterned surface against nonspecific adherence, after which the baseline photocurrent distribution was measured. The sample was then immersed in a solution containing anti-HspX antibody (200 ng/ml) for 1 h to allow the antibody to bind to the immobilized HspX on the LEAC biosensor, followed again by photocurrent measurements. Although fluorescent labeling is not required for LEAC biosensing, to confirm the location of HspX, the LEAC sensor was then submerged in fluorescent-labeled antimouse IgG solution for 1 h to mark the presence of the anti-HspX spot [Fig. 3(a)].

As shown in Fig. 3(a), HspX was printed on detectors 4 to 7, and antigen 85 was printed on detectors 10 to 13. After incubation with an HspX-specific antibody, an 8% maximum modulation ratio was observed, which corresponds to a 0.5 nm change in average nanobiofilm thickness. No significant change in photocurrent was detected in the location where Ag85 was printed, indicating specificity of the anti-HspX antibody for the HspX antigen. Subsequent incubation with Cy3-labeled antimouse IgG resulted in specific binding to the captured anti-HspX, and caused an additional 5% current decrease on detector 6. These results show the LEAC

biosensor can be used to selectively detect specific TB antibodies.

The ac measurement system described above was used for the TB antigen/antibody immunoassay to improve the metrology limit. 30 measurements were made with a lock-in time constant of 300 ms, requiring a total acquisition time of 10 s to obtain the current on each detector. The ac measurements improved the metrology limit to 0.22% corresponding to 14 pm while also removing the requirement for separate light and dark measurements. However, the modulation ratios measured on detectors 5 and 6 after exposure to anti-HspX were much more variable than those in the anti-IgG experiment. Nonuniform anti-HspX distribution in the patterned region led to a LOD calculated from the two detectors that is larger than the average modulation ratio. Improvements in HspX antigen and antibody immobilization are thus needed to significantly reduce the LOD of the LEAC sensor for applications in TB serology.

In this study, LEAC biosensor performance for label-free immunoassays was evaluated. Photocurrent modulation in response to various antibody-antigen interactions was measured using buried detector arrays. Modulation ratios of 16.3% and 3.5% were observed in response to mouse IgG antibody and antigen patterning, respectively. In a separate experiment, the *M. tuberculosis* protein antigens HspX and Ag85 were used to successfully test the specificity of the LEAC biosensor. A metrology limit of 28 pm for dc measurements was reduced by half to 14 pm using ac measurements. Using a dried protein density of 1.41 g/ $\text{cm}^3$ , for large molecules,<sup>15</sup> the ac metrology limit corresponds to 20 pg/ $\text{mm}^2$ . Based on the variation of adjacent detector modulation, the limit of detection of the LEAC sensor is 87 pm (120 pg/ $\text{mm}^2$ ) for the goat antimouse IgG patterning and 108 pm (150 pg/ $\text{mm}^2$ ) for the bound mouse IgG layer. A poor LOD for the HspX immunoassay was attributed to nonuniform nanobiofilm thickness, which should be improved to allow use of the LEAC biosensor as a compact low cost point of care diagnostics for *M. tuberculosis* and other medically important pathogens.

<sup>1</sup>K. Dheda, S. K. Schwander, B. D. Zhu, R. N. van Zyl-Smit, and Y. Zhang, *Respirology* **15**, 433 (2010).

<sup>2</sup>N. Prabhakar, K. Arora, S. K. Arya, P. R. Solanki, M. Iwamoto, H. Singh, and B. D. Malhotra, *Analyst (Cambridge, U.K.)* **133**, 1587 (2008).

<sup>3</sup>Q. Q. Gan, Y. K. Gao, and F. J. Bartoli, *Opt. Express* **17**, 20747 (2009).

<sup>4</sup>Y. Q. Luo, F. Yu, and R. N. Zare, *Lab Chip* **8**, 694 (2008).

<sup>5</sup>K. De Vos, I. Bartolozzi, E. Schacht, P. Bienstman, and R. Baets, *Opt. Express* **15**, 7610 (2007).

<sup>6</sup>R. Yan, S. P. Mestas, G. W. Yuan, R. Safaisini, D. S. Dandy, and K. L. Lear, *Lab Chip* **9**, 2163 (2009).

<sup>7</sup>G. W. Yuan, M. D. Stephens, D. S. Dandy, and K. L. Lear, *IEEE Photonics Technol. Lett.* **17**, 2382 (2005).

<sup>8</sup>M. D. Stephens, G. Yuan, K. L. Lear, and D. S. Dandy, *Sens. Actuators B* **145**, 769 (2010).

<sup>9</sup>R. Yan, G. W. Yuan, M. D. Stephens, X. Y. He, C. S. Henry, D. S. Dandy, and K. L. Lear, *Appl. Phys. Lett.* **93**, 101110 (2008).

<sup>10</sup>R. Yan, S. P. Mestas, G. W. Yuan, R. Safaisini, and K. L. Lear, *IEEE J. Sel. Top. Quantum Electron.* **15**, 1469 (2009).

<sup>11</sup>X. Wang, M. Zhao, and D. D. Nolte, Proceedings of The Conference on Lasers and Electro-Optics 2010 (CLEO 2010), 2010.

<sup>12</sup>A. Bernard, B. Michel, and E. Delamar, *Anal. Chem.* **73**, 8 (2001).

<sup>13</sup>M. J. Sartain, R. A. Slayden, K. K. Singh, S. Laal, and J. T. Belisle, *Mol. Cell. Proteomics* **5**, 2102 (2006).

<sup>14</sup>P. Wu, P. Hogrebe, and D. W. Grainger, *Biosens. Bioelectron.* **21**, 1252 (2006).

<sup>15</sup>H. Fischer, I. Plikarpov, and A. F. Craievich, *Protein Sci.* **13**, 2825 (2004).